ELSEVIER

Nuclear Instruments and Methods in Physics Research A 440 (2000) 462–465

NUCLEAR INSTRUMENTS & METHODS IN PHYSICS RESEARCH Section A

www.elsevier.nl/locate/nima

Letter to the editor

Improving the energy resolution of a hemispherical spectrograph using a paracentric entry at a non-zero potential

E.P. Benis, T.J.M. Zouros*

Department of Physics, University of Crete, P.O. Box 2208, 71003 Heraklion, Crete, Greece

Received 17 August 1999

Abstract

We demonstrate by ray tracing analysis that the focusing properties of a hemispherical spectrograph depend critically on the placement of the electron entrance position R_0 and the value of the potential V_0 at R_0. Improvements over conventional spectrographs using $R_0 = \bar{R}$, the mean radius and $V_0 = 0$ are predicted for particular combinations of R_0 and V_0. A spectrograph with $\bar{R} = 101.6$ mm and an entrance at $R_0 = 82.55$ mm using a zoom lens and a two-dimensional position sensitive detector (2D-PSD) with 40 mm multichannel plates and resistive anode encoder has been used to confirm the predicted qualitative behaviour. These results suggest that improvement in energy resolution may be attained without the use of fringing field correctors. © 2000 Elsevier Science B.V. All rights reserved.

PACS: 39.30 + w; 7.81 + a

Keywords: Electron spectroscopy; Hemispherical spectrometers; Fringing field corrections; Position-sensitive detectors; ESCA

The properties of hemispherical analysers and their operation have been extensively described in the literature for slit spectrometers (see for example the recent review by Roy and Tremblay [1] and references therein) and to a lesser extent for spectrographs [2–4], where the exit slit has been replaced by a positive-sensitive detector (PSD). Conventional hemispherical analysers are used with an entrance aperture centered at a radial distance $R_0 = \bar{R}$, where $\bar{R} = \frac{1}{2}(R_1 + R_2)$ is the mean radius. Furthermore, the entrance potential at R_0 is usually set at 0, i.e. $V_0 \equiv V(R_0) = 0$. Then the central ray trajectory is a circle.

However, when the fractional inter-radial separation $\rho = \Delta R/\bar{R}$ is large, such as in the case of modern day spectrographs using PSDs (here $\rho = 0.575$), the effect of the entrance and exit fringing fields can result in large departures from the $1/r$ potential dependence of an ideal spherical condenser. This usually results in a shift of the focus of the spectrograph from the exit plane at a deflection angle of 180° to some smaller deflection angle inside the analyser with a corresponding loss in energy resolution. Various correction schemes have been proposed [6], the most common solution (albeit cumbersome) being the use of multiple rings or

* Corresponding author. Tel.: 30-81-394117; fax: 30-81-314101.

E-mail address: tzouros@physics.uch.gr (T.J.M. Zouros)

0168-9002/00/$ - see front matter © 2000 Elsevier Science B.V. All rights reserved.
PII: S0168-9002(99)00954-7

strips to terminate the electric field at the ends of the hemispherical electrodes [2,7]. Here, we demonstrate by ray tracing calculations, performed with the popular ion-optics package SIMION, that improved focusing over conventional spectrographs using $R_0 = \bar{R}$ and $V_0 = 0$ are predicted for particular combinations of R_0 and V_0. These results suggest that good energy resolution may be attained without the use of fringing field correctors for paracentric entry ($R_0 \neq \bar{R}$) simplifying the implementation of large area PSDs.

A high gain, paracentric, ESCA-like electron spectrometer has recently been set-up [8–10] for use in zero-degree Auger spectroscopy of ions in energetic collisions with atoms. Such measurements take place at an observation angle of 0° with respect to the beam direction to minimize an otherwise large kinematic broadening seriously degrading energy resolution [11]. The spectrograph (see Refs. [8,9] for a figure of the experimental setup) is composed of a conventional hemispherical analyser, a 4-element focusing lens system (zoom lens) and a two-dimensional position sensitive detector (2D-PSD), all commercially available. The hemispherical shells have an outer radius $R_2 = 130.8$ mm and inner radius $R_1 = 72.4$ mm. The large inter-radial distance $\Delta R = R_2 - R_1 = 58.4$ mm easily accommodates a 40 mm 2D-PSD allowing for a detection energy window of 20% around the central energy. The zoom lens provides two important functions: (a) It focuses the incoming electrons at the entrance of the analyser, thus simulating a small virtual slit necessary for high-resolution measurements. This is particularly important in our application at 0° observation angle (where the primary ion beam has to pass through the analyser itself) since small apertures lead to severe electron background from slit scattering of the primary ion beam. An entrance aperture of 6 mm diameter was used for this reason. (b) It decelerates projectile electrons, typically in the energy range of a few keV, down to a few hundreds of eV for improved resolution.

The trajectory equations within an *ideal* spherical condenser are only known for the case of central entrance at $V_0 = 0$, to the best of our knowledge. We thus had to solve the problem of *arbitrary* entrance R_0 and potential V_0 from basic principles. In this case the trajectory of the central ray is an ellipse. In Table 1 we summarize some of the important differences between central and paracentric (off-central) entrance for the *ideal* hemispherical analyser. The full treatment will be presented elsewhere [12]. From the general trajectory equation the voltages V_i can be determined analytically (see Table 1). They are seen to be functions of the energy T_0 of the central ray used to "tune" the analyser and the potential V_0 which is used as a free parameter and adjusted for best results. In the case of the ideal condenser $V_0 = V(R_0)$ with $V(r)$ the $1/r$ potential inside the analyser. Clearly fringing field effects are *not* included in such a treatment.

To include the fringing field effects we use the ion-optics package SIMION 3D [5]. In Fig. 1 we compare two identical spectrometers, for central ($R_0 = \bar{R} = 102$ mm) and paracentric ($R_0 = 82$ mm) electron entry. In both cases, all voltages on lens and hemispheres ($V_1 = 877.5$ V and $V_2 = -503.5$ V) are the same. The lens focuses the electrons at the entrance of the analyser. The $V = 0$ equipotential is emphasized. The result of the fringing fields

Table 1
Basic features of an *ideal* hemispherical electron analyser for central and paracentric entry. The mean radius of the analyser is $\bar{R} = \frac{1}{2}(R_1 + R_2)$. The exit point of the central ray in both cases has been chosen for central exit on the PSD at $\bar{R}$

	Central entry	Paracentric entry
Entrance point R_0	$R_0 = \bar{R}$	$R_1 < R_0 < R_2$
Central ray trajectory	Circle	Ellipse
Entrance potential V_0	$V_0 = 0$	$V_2 < V_0 < V_1$
Analyser voltages V_i ($i = 1,2$)	$2\left(\frac{\bar{R}}{R_i} - 1\right)T_0$	$\frac{R_0}{R_i}\left[1 + \frac{(R_0 - R_i)}{\bar{R}}\right]V_0 + \left(1 + \frac{R_0}{\bar{R}}\right)\left(\frac{R_0}{R_i} - 1\right)T_0$

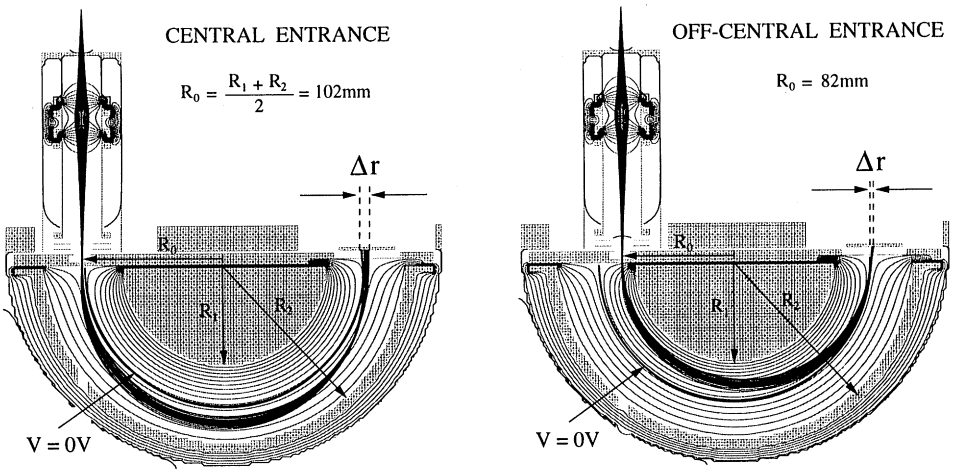

Fig. 1. SIMION simulation. Electrons with initial kinetic energy $T_0 = 1000$ eV are flown from a point source located at a distance of 30 mm from the lens entrance within an emittance cone angle of 6°. These are focused at the entrance of the analyser by the lens. Left: central entrance with $R_0 = \bar{R} = 102$ mm and $V_0 = 0$. Right: paracentric (off-central) entrance with $R_0 = 82$ mm and $V_0 \approx 500$ V. In both cases all voltages are the same. Clearly observable are the improved focusing conditions on the position sensitive detector achieved for the paracentric entrance.

on the potential near the entrance and the exit of the analyser are clearly visible. For the case of central entry, the well-known shifting of the focus from the exit plane at the deflection angle $\theta = 180°$ to smaller deflection angles is clearly seen to result in a badly focused trace Δr. In the paracentric case good focusing conditions on the detector plane are restored.

In Fig. 2 (left) we plot the base energy resolution $R_b = \Delta E/E$ as a function of V_0 for different entry values of R_0. These results were also obtained by SIMION. In each case we used the same group of electrons as those shown in Fig. 1. These were flown in SIMION and their trace width Δr across the PSD was recorded. An energy calibration was used to convert Δr to the base energy width ΔE. The energy calibration was accomplished with SIMION by flying electrons with different energies and recording their position on exit along the PSD. Voltages were set using the equations for V_i from Table 1. In a similar way, the overall energy acceptance window ΔT_{window} was determined for each case and displayed in Fig. 2 (right). The limiting values of the energy window were defined by the limits of the analyser inner walls. Only energies which resulted in 100% transmission through the analyser were used for the determination of ΔT_{window}, which explains the sudden cut-off of the values in the graphs.

As can be seen directly from Fig. 2, there is no one entrance position which gives best resolution. Rather, specific combinations of R_0 and V_0 lead to the best focusing conditions. Thus, for $R_0 = 82$ mm, a voltage of $V_0 = 0.6T_0$ is seen to give the best energy resolution. However, for a conventional analyser having $R_0 = \bar{R} = 102$ mm, SIMION indicates that the energy resolution is best for $V_0 = 0$ with the resolution getting *worse* with increasing values of V_0. We also note that the energy window of the analyser becomes larger as R_0 increases and V_0 decreases.

We are in the process of verifying these SIMION results experimentally. Indeed, our paracentric spectrograph (with lens focused) having its entrance at $R_0 = 82.55$ mm, showed a similar dependence on V_0 as that of Fig. 2 (left) attaining its best FWHM energy resolution (0.9% without deceleration) for $V_0 = 0.46T_0$ with an acceptance window of about $0.2T_0$. This small difference from the SIMION prediction of $0.6T_0$ could be due to differences in the focusing of the lens which cannot be monitored in the experiment.

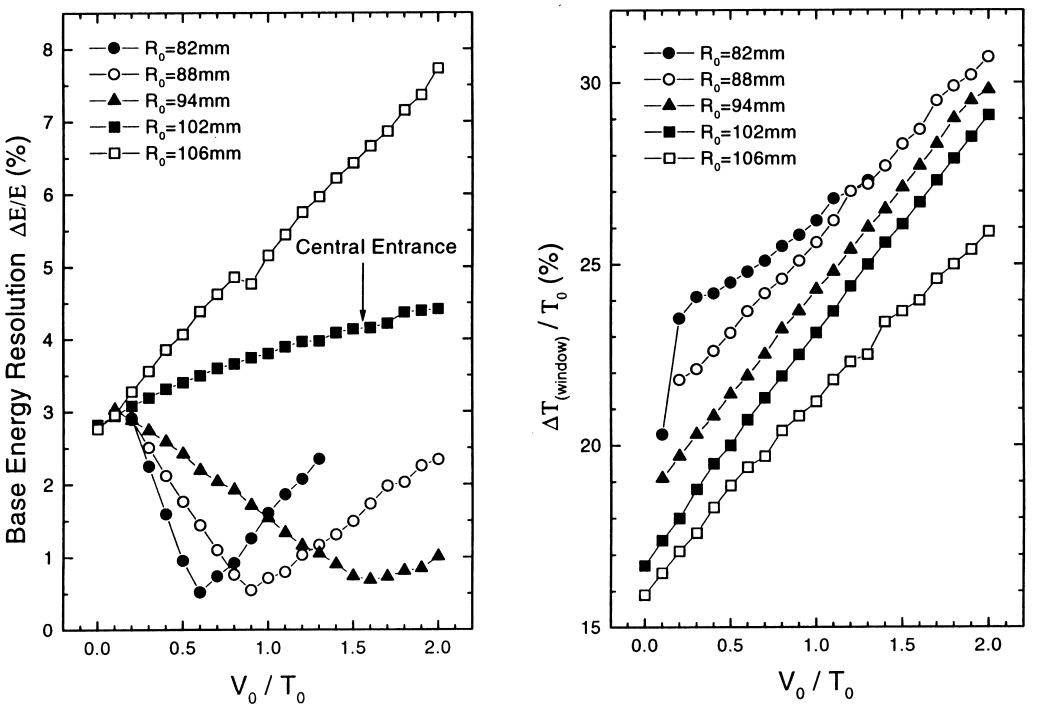

Fig. 2. Base energy resolution (left) and acceptance energy window (right) for a hemispherical spectrograph with different locations of the entry point R_0 and entrance potential parameter V_0. Only cases where the transmission through the analyser was 100% were considered.

In conclusion, we have performed ray tracing calculations which indicate that improved focusing can be attained for particular combinations of entrance position R_0 and entrance potential parameter V_0 which differ from the conventional hemispherical spectrograph settings of $R_0 = \bar{R}$ and $V_0 = 0$. Experimental results supported the predicted behaviour for $R_0 = 82.55$ mm.

We acknowledge partial support by the Division of Chemical Sciences, Office of Basic Energy Sciences, Office of Energy research, US Department of Energy and the Greek Ministry of Research and Technology (PENED95 grant). We would also like to thank Dave Dahl, author of SIMION, for his generous help.

References

[1] D. Roy, D. Tremblay, Rep. Prog. Phys. 53 (1990) 1621 and references therein.
[2] F. Hadjarab, J. Erskine, J. Electron. Spectrosc. Rel. Phenom. 36 (1985) 227 and references therein.
[3] B. Gurney, W. Ho, L.J. Richter, J. Villarrubia, Rev. Sci. Instr. 59 (1988) 22 and references therein.
[4] P. Hayes, M. Bennett, J. Flexman, J. Williams, Rev. Sci. Instr. 59 (1988) 2445 and references therein.
[5] D.A. Dahl, SIMION 3D v6.0, Idaho National Engineering Laboratory, Idaho Falls, 1996.
[6] D. Hu, K. Leung, Rev. Sci. Instr. 66 (1995) 2865 and references therein.
[7] E.-J. Jeong, J. Erskine, Rev. Sci. Instr. 60 (1989) 3139 and references therein.
[8] E.P. Benis, K. Zaharakis, M.M. Voultsidou, T.J.M. Zouros, M. Stöckli, P. Richard, S. Hagmann, Nucl. Instr. and Meth. B 146 (1998) 120.
[9] E.P. Benis, T.J.M. Zouros, P. Richard, Nucl. Instr. and Meth. B 154 (1999) 276.
[10] E.P. Benis, T.J.M. Zouros, H. Aliabadi, P. Richard, Phys. Scripta T80B, 529–531 (1999).
[11] T.J.M. Zouros, D.H. Lee, in: S.M. Shafroth, J.C. Austin (Eds.), Accelerator-Based Atomic Physics Techniques and Applications, American Institute of Physics Conference Series, New York, 1997, pp. 426–479.
[12] E.P. Benis, T.J.M. Zouros, in preparation.